Characterizing Indoor Wireless Channels via Ray Tracing, and Validation via Measurements

Aliye Özge Kaya, Larry Greenstein, Wade Trappe
WINLAB, Rutgers University, Technology Centre of New Jersey
671 Route 1 South, North Brunswick, NJ 08902-3390
{ozgekaya, ljg, trappe}@winlab.rutgers.edu

***Abstract*—We investigate the reliability of radio channel simulators in capturing the important properties of radio channels throughout a well-specified environment. Indoor environments for which the geometric layout and material properties of surfaces are known lend themselves to such site-specific simulation. Our aim is to assess the performance of this approach by comparing its predictions with measurements in a specific environment. The measurements are made on 18 paths in the ORBIT Laboratory of Rutgers University's WINLAB; and the simulator we use is the WiSE ray-tracing tool developed by Bell Labs. The comparisons are made for three parameters that largely characterize a radio path's behavior: Path loss; Ricean K-factor; and RMS delay spread. The measurements are made over a 1-GHz bandwidth centered on 3.5 GHz. The comparisons show good agreement over the set of paths measured and simulated, establishing confidence that a well-designed radio simulator can be used reliably in system studies.**

I. Introduction

In wireless communications, the underlying radio channel properties strongly affect the performance of the system. It is common practice in design and evaluation studies of such systems to use mathematical models for describing the channel. One approach is stochastic modeling, in which the key properties of the signal propagation (e.g., multipath fading) are captured by probability distributions. These kinds of models are favored when the propagation environment is unknown except for some high-level attributes, e.g., urban vs. suburban, flat vs. hilly, summer vs. winter, etc.

Stochastic models serve well when the study questions are fairly generic, e.g., how does a particular cellular radio system perform in an environment that is typically urban? However, there are cases where the interest pertains to a specific environment, e.g., a wireless LAN in the corporate offices of a specific company. In such cases, the study questions are 'site-specific' and so site-specific channel response information is needed. One very effective approach in that case might be to measure channel responses for a very large population of transmit-receive (T-R) paths and store them in a database that can be accessed for system simulations. The number of such paths that must be sampled, however, can be extremely large and require measurement campaigns that are long, labor-intensive and costly.

An alternative that is less precise in terms of channel description but also far less costly is to use *environment simulators*. These are computer programs that (1) emulate the physical environment; and (2) use wave propagation physics to predict the radio signal produced at any receive point from any transmit point. When the physical environment is well-specified, such as indoor areas where the layouts and materials of walls, floors and ceilings are known, environment simulation can be employed on a very large scale with very little effort. The question is whether such simulation tools reliably capture the radio channel behaviors in the specified environment.

It is axiomatic that no typical environment can be perfectly emulated. Propagating radio signals will be affected by countless artifacts that are hard to capture and/or predict, i.e., moldings, variations in material, furniture, etc. What can reasonably be expected, however, is that a site-specific program predicts channel responses throughout the area of interest that are statistically similar to the actual ones. To this end, we can cite three parameters of a radio path that go a long way to describing its response for both narrow and wide bandwidths. They are (1) the *path loss*, *PL*, which is the dB value of the transmit power divided by the (locally averaged) received power; (2) the *Ricean K-factor*, which, together with PL, dictates the narrowband fading distribution; and (3) the *RMS delay spread*, τ_{rms}, which is a measure of the frequency selectivity (or pulse dispersion) of the channel. We assert that a site-specific program that accurately predicts these three quantities throughout a specified environment can be relied upon in conducting radio performance studies for that environment.

In this paper, we consider a particular environment, namely, the ORBIT Laboratory of Rutgers University's WINLAB [1], [2]; and we test a particular simulator, namely, the Wireless Systems Engineering (WiSE) Tool, a ray-tracing program developed by Bell Labs [3]. For a total of 18 chosen T-R paths, we use a Vector Network Analyzer (VNA) to measure complex frequency responses over a wide bandwidth, i.e., from 3 to 4 GHz; and we use WiSE to predict the path loss, K-factor and RMS delay spread. The good agreement between VNA data and WiSE predictions in most cases establishes confidence that a well-designed simulator can be effective in capturing the radio channel properties of a specified environment. Our investigation underscores the importance of accurately specifying the electrical properties of the surfaces (walls, etc.) in addition to their layouts.

The paper is organized as follows. In Section II, we explain the measurement and simulation methodology that is used

throughout this paper. Section III explains the K factor estimation methods from impulse and frequency responses. Section IV gives a brief overview of RMS delay spread. Section V compares WiSE predictions with the VNA measurement in terms of path gain, K factor and RMS delay spread. Section VI concludes the paper.

II. Methodology

A. Measurements with a Vector Network Analyzer (VNA)

In our experiments, we measured the complex channel response with the vector network analyzer (VNA) Agilent E5071B. Measurements were carried out at various locations in the ORBIT room of WINLAB, Rutgers University. The ORBIT room is of size 20 m$\times$25 m and it is surrounded by offices, cubicles and hallways. All antennae were at the same height, 1.25 m, and all transmit powers were 10 dBm. The VNA measured the complex frequency response at M equally spaced frequencies over a given frequency range.

Specifically, we measured the complex frequency response at 1601 points between 3 and 4 GHz for various transmitter-receiver paths. We repeated this VNA experiment 50 times for each path. Since the differences among the experiments were small, we show the results for only one of each path measurement. We chose the frequency range as the 3 and 4 GHz to avoid interference from the widely used 2.4 and 5 GHz bands.

B. Simulations with the WiSE Tool

We used WiSE [3] to simulate the radio environment of the same room where we conducted our VNA measurements. Given a building plan and transmitter location, WiSE simulates the signals received at any point in the building, as illustrated in Figure 1 for one receiver location. It accounts for the many rays that undergo reflection and transmission, where the number of reflections included per ray is a program input. It takes into account path loss and the wall layer properties, such as dielectric coefficient, width, conductivity, number of layers, etc. In WiSE each wall is defined by its geometric layout and by a parameter called 'wall type'. An existing wall type can be redefined or a new wall type can be defined by declaring the dielectric coefficients, width, conductivity for each layer of the wall.

III. K-factor Estimation Methods

A. Prior Work on Ricean K-factor Estimation

The K-factor is usually the ratio of the power in the line of sight (LOS) component to the total power of the non-LOS (NLOS) components. It is a measure of the extent of fading on the link, where lower K means deeper fading.

Various algorithms has been proposed to estimate the K factor. The moment method [4] estimates the K factor from the second and fourth moments of the signal fading variation over time, space or frequency. It is more practical than many other proposed methods. The moment method can be generalized to use with different moments, as in [5]. The authors in [5] also propose a K factor estimation method using the in-phase and quadrature components, but this method is applicable only to narrow band signals. The method of maximum likelihood (ML) estimation of K-factor is proposed in [6], wherein the parameters of the Ricean distribution are chosen as those parameters which maximize the joint probability density of the observed outcomes.

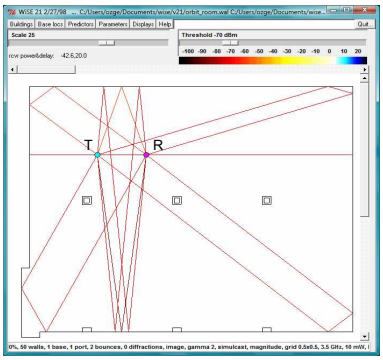

Fig. 1. Rays generated by WiSE for the transmitter location T and receiver location R

B. Estimation from Impulse Responses

The channel impulse response gives the rays received at different delays. The ray which has the largest magnitude is designated as the "LOS" component. The power sum of the other remaining rays constitute the "scatter" power. The ratio of the LOS ray's power to the scatter power gives the K-factor. This is perhaps the simplest way to estimate the K factor.

Note that the physical LOS component is almost always the one with the shortest delay. Thus, the power we use for the K-factor numerator may or may not be the actual LOS power. From the standpoint of estimating a K factor that accurately predicts the fading distribution, however, this is an intuitive approach that (as we will show) leads to excellent results.

C. Estimation from Frequency Responses (Coherent Method)

The K factor can be also computed from complex frequency response coherently. Assume we know the complex channel response $H(f)$ at M different frequencies. Let $V = |V|e^{-j\phi}$ be the complex amplitude of the LOS component. It can be estimated by minimizing the difference between the expected and measured channel response. Thus,

$$V^* = \arg\min_V E_f\{|H(f) - |V|e^{-j(2\pi f\tau+\phi)}|^2\} \quad (1)$$

where τ is the delay at which the LOS component is received. The solution to this minimization problem V^* is

$$V^* = E_f\{H(f)e^{j2\pi f\tau}\} \quad (2)$$

where τ is found as

$$\tau^* = \arg\max_\tau E_f\{|H(f)e^{j2\pi f\tau}|\} \quad (3)$$

This solution is equivalent to performing an inverse Fourier transform on the frequency domain data and choosing the largest component as the LOS component. Therefore, the

coherent method gives the same result as estimating the numerator of the K-factor from the most powerful ray of the impulse response.

D. Estimation from Frequency Responses (Moment Method)

The moment method was first proposed in [4] assumed a temporal variation of the received signal. It uses the second and fourth moments of the variation over some long interval for the K-factor estimation. This method needs only the absolute values of the received signal samples. It is also applicable to frequency domain data, assuming a very wide bandwidth. Thus, the K-factor can be computed by computing second and fourth moments from the samples of $|H(f)|$.

This method loses precision at very low K-factors, i.e., $K \leq 1$. At the same time, the fading distribution does not change much over that range of K, so that imprecision in estimating K is not essential.

IV. RMS Delay Spread

The RMS delay spread is a measure of the frequency selectivity (or pulse dispersion) of a link. Pulse dispersion arises as a result of the signals taking different times to cross the channel through different propagation paths. RMS delay spread is defined as the second central moment of the power delay profile:

$$\tau_{rms} = \sqrt{\bar{\tau^2} - \bar{\tau}^2} \tag{4}$$

where

$$\bar{\tau} = \frac{\sum_{i=1}^{N} P_i t_i}{\sum_{i=1}^{N} P_i} \quad \bar{\tau^2} = \frac{\sum_{i=1}^{N} P_i t_i^2}{\sum_{i=1}^{N} P_i} \tag{5}$$

N is the number of received rays; and P_i and t_i are, respectively, the power and arrival time of i^{th} ray. Setting (5) into (4) it can be shown that,

$$\tau_{rms} = \frac{1}{\sum_{i=1}^{N} P_i} \sqrt{\sum_{i=1}^{N} \sum_{j=1+i}^{N} P_i P_j (t_i - t_j)^2} \tag{6}$$

We can rewrite (6) as

$$\tau_{rms} = \sqrt{\sum_{i=1}^{N} \sum_{j=1+i}^{N} \rho_i \rho_j (t_i - t_j)^2} \tag{7}$$

where ρ_x is the normalized power of x^{th} ray

$$\rho_x = \frac{P_x}{\sum_{i=1}^{N} P_i} \tag{8}$$

where $0 \leq \rho_x \leq 1$. From (7) it is obvious that RMS delay spread depends only on delay differences, and does not depend on where we set the origin, $\tau = 0$. It also does not depend on the transmit power, but solely on the power ratios of the rays.

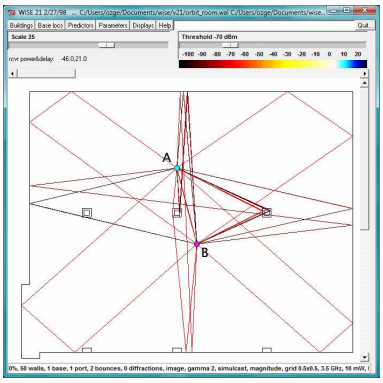

Fig. 2. Rays generated by WiSE for the transmitter location A and receiver location B

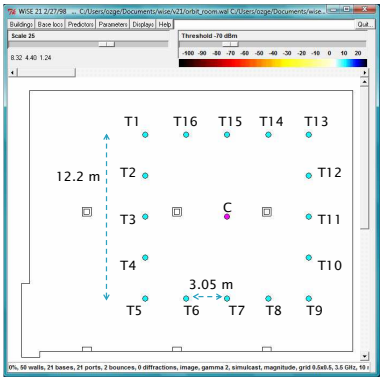

Fig. 3. Receiver Location C and transmitter locations T1 to T16

V. Comparing VNA Data and WiSE Predictions

A. Transmitter-Receiver Paths Measured

We will report on VNA-WiSE comparisons for 18 different transmitter-receiver paths. We repeated such experiments for various other paths and found similar results. Figure 1 shows the transmitter-receiver path $T \rightarrow R$, where T and R are 3.7 m apart. Figure 2 shows the transmitter and receiver path $A \rightarrow B$, where A and B are 5.8 m apart. Figure 3 shows the receiver location C and the transmitter locations $T1$ to $T16$, located on a square of size 12.2 m x 12.2 m. Neighboring transmitter locations are about 3 m apart.

B. Wall Properties

The walls in the ORBIT room are made of multiple layers of different materials used for isolation and shielding. Moreover, not every wall has the same layers; and we do not have exact information on the properties of these layers. Therefore, modeling of the walls is not straightforward. We considered for each wall various predefined wall types in WiSE. We have chosen those wall types for which preliminary experiments and comparisons between VNA and WiSE results showed the best agreement. For the ceiling and floor we chose a concrete wall type, for the other walls, we chose metallic and sheetrock wall types. The pillars on the radio path cause diffraction, reflection

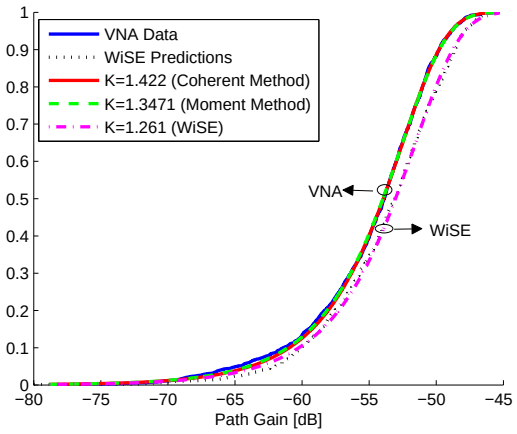

Fig. 4. Comparison of CDF's of path gain ($T \rightarrow R$) The curves shown with K factor are the Ricean CDFs. The VNA-derived, and WISE-predicted CDFs look like one another and the Ricean CDFs.

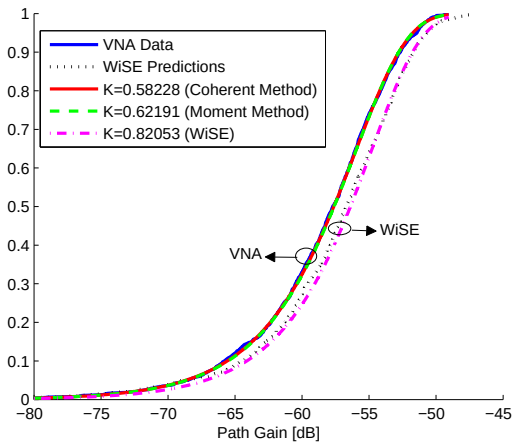

Fig. 5. Comparison of CDF's of path gain ($A \rightarrow B$) The same comments apply as in Figure 4.

and transmission which affect the received power significantly. Therefore, accurate modeling of the pillars is necessary. We modeled the pillar walls using a sheetrock wall type. We know that each pillar is built with a metallic block inside. Therefore, we added a second layer of walls made of metal inside the pillars. During our search for the best wall type combinations, we learned how critical the electrical properties of the walls are in addition to their geometry. We conclude that a certain amount of preliminary trial-and-error (measurement, comparison and adjustment) is needed for the prediction tool to be confidently applied.

C. Path Gain, K-factor and Fade CDF's

The cumulative distribution function (CDF) of the path gain can be obtained directly by sorting the measured or simulated channel response samples. We call this the empirical CDF. A good fit to this curve is the theoretical Ricean CDF, parameterized only by the K factor and average power gain.

Figures 4 and 5 compare the CDF's for path gain for the paths $T \rightarrow R$ and $A \rightarrow B$. We see that the theoretical curves (obtained for K-factors estimated using either the moment method or the impulse response method) are very good matches to the empirical CDF's. Also, the WiSE-based and VNA-based CDF's of path gain are very close to each other.

Figure 6 shows the variation of the average path gain and Figure 7 shows the variation of the K factor among the links $T1 \rightarrow C$ to $T16 \rightarrow C$. In both figures measured and predicted values show good agreement. Additionally, our results show that in indoor environments K factor is very low due to the transmissions and reflections with the walls and objects in the surrounding. The maximum K factor in this experiment was 1.13.

D. RMS Delay Spread

The RMS delay spread, τ_{rms}, depends solely on the delay differences among the rays and on their relative powers, (7).

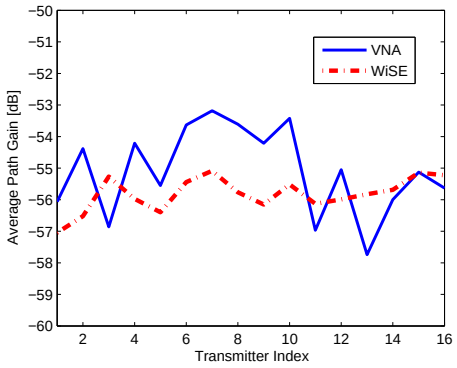

Fig. 6. Power gain comparison at the locations $T1 \rightarrow C$ to $T16 \rightarrow C$

Because the delay spread is based on moments of a function, impulse response rays at the larger delays can have an important impact on the calculated result, even if their powers are very low. The VNA-derived impulse response, being an inverse Fourier transform of measured frequency response samples, has rays out to a maximum delay dictated by the measurement bandwidth (1 GHz) and the number of samples (1601), i.e., out to 1.6 μs. This is much larger than the actual maximum delay in an indoor environment. The additional 'rays' in the VNA-derived impulse response are the result of measurement noise and other measurement impairments.

To fairly compare the VNA-derived τ_{rms} with the value predicted using WiSE, we should use a maximum delay, t_η, that is common to both calculations. We chose the delay at which the WiSE ray powers drops permanently below -30 dB relative to the strongest ray in the impulse response. Thus, from both the VNA-derived and WiSE-predicted impulse responses, we calculate RMS delay spread using rays from relative delay 0 to relative delay t_η.

The RMS delay spreads for the transmitter locations T1 to T16 using the two methods are shown and compared in

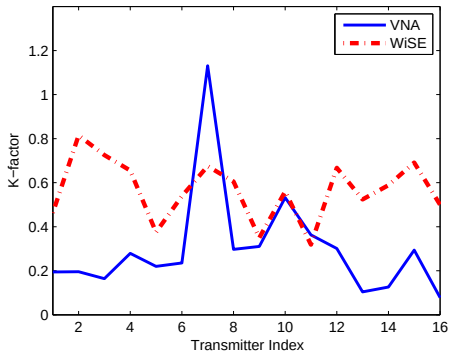

Fig. 7. K factor comparison at the locations $T1 \rightarrow C$ to $T16 \rightarrow C$

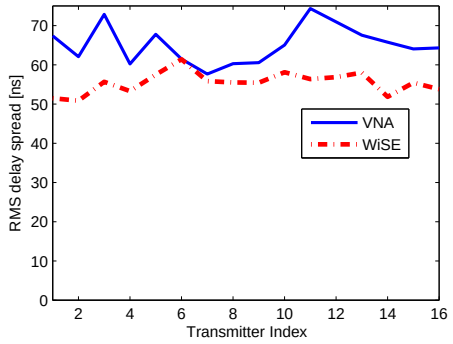

Fig. 8. RMS delay spread comparison at the locations $T1 \rightarrow C$ to $T16 \rightarrow C$

Figure 8. They differ in most cases by 20 percent or less, with the VNA-derived estimates always being higher. In just a few cases, the VNA-derived value is up to 30 percent higher.

The consistent increase of VNA-derived values over WiSE predictions may be due to imperfect calibration of the VNA data. The VNA-derived delay spread can be shown to be sensitive to calibration errors, and in a way that would increase its estimated value (c.f., [7]). Correcting for this impairment would improve the comparisons shown. This possibility bears further study.

VI. Further Discussion and Conclusion

Table I summarizes the measured and predicted values of K-factor, average path gain and RMS delay spread for the 18 paths we studied, Figs. 1-3. The parameters predicted using WiSE agree well with measurements over this set of paths. This suggests, at the very least, that a well-designed ray-tracing program such as WiSE can be used with confidence for studying systems in wireless environments like the ORBIT Lab.

In the course of our investigation, we identified two conditions that can compromise prediction accuracy of critical path properties: (1) Paths where diffraction is the primary propagation mechanism; and (2) environments for which the material properties of the walls, floor and ceiling are not well-specified. The first condition is relatively rare in indoor environments; the second condition can be avoided by using a small number of preliminary measurements, augmented by comparisons with predictions and corresponding adjustments of the assumed material properties.

Further work in this area should include, primarily, its extension to other paths and to other indoor environments. In addition, a limited amount of system studies would help to test the conjecture that the parameters studied here (path gain, K-factor and RMS delay spread) comprise a sufficient set for capturing the properties of a channel response. It would also be useful to establish that the agreements shown here are sufficiently good to vindicate the use of ray-tracing tools in place of labor-intensive measurements.

Acknowledgements

We are grateful to Dmitry Chizhik, Jonathan Ling and Reinaldo Valenzuela, all of Alcatel-Lucent, for many fruitful discussions on the uses of the WiSE tool.

References

[1] J. Lei, R. Yates, L. Greenstein, and H. Liu, "Mapping link SNRs of wireless mesh networks onto an indoor testbed," *Conf. Rec. of TridentCom*, March 2006.

[2] M. Ott, I. Seskar, R. Siracusa, and M. Singh, "ORBIT Testbed Software Architecture: Supporting experiments as a service," *Proceedings of IEEE Tridentcom*, Feb 2005.

[3] S. Fortune, D. Gay, B. Kernighan, O. Landronand, R. Valenzuela, and M. Wright, "WISE design of indoor wireless systems: practical computation and optimization," *IEEE Computational Science and Engineering*, vol. 2, no. 1, pp. 58–68, 1995.

[4] L. Greenstein, D. Michelson, and V. Erceg, "Moment method estimation of the Ricean K-factor," *IEEE Communication Letters*, vol. 3, pp. 175–176, June 1999.

[5] C. Tepedelenlioglu, A. Abdi, and G. Giannakis, "The Ricean K Factor: Estimation and Performance Analysis," *IEEE Trans. Commun.*, vol. 2, pp. 799–809, July 2003.

[6] K. Talukdar and W. Lawing, "Estimation of the parameters of the Rice distribution," *J. Acoust. Soc. Am.*, vol. 89, no. 3, pp. 1193–1197, March 1991.

[7] A. Saleh and R. Valenzuela, "A statistical model for indoor multipath propagation," *IEEE J. Sel. Areas Commun.*, vol. 5, no. 2, pp. 128–137, Feb 1987.

TABLE I
Comparision WiSE and VNA data

	Av. Path Gain [dB]		**K**		**RMS d. s. [ns]**	
	VNA	WiSE	VNA	WiSE	VNA	WiSE
T→R	-53.01	-52.04	1.42	1.26	41	34
A→B	-56.29	-55.18	0.58	0.82	58	48
T1→C	-56.07	-57.05	0.19	0.46	67	52
T2→C	-54.38	-56.52	0.20	0.82	62	51
T3→C	-56.86	-55.27	0.16	0.73	73	56
T4→C	-54.21	-55.97	0.28	0.66	60	53
T5→C	-55.55	-56.40	0.22	0.38	68	57
T6→C	-53.63	-55.44	0.24	0.54	61	61
T7→C	-53.18	-55.08	1.13	0.68	58	56
T8→C	-53.60	-55.76	0.30	0.61	60	56
T9→C	-54.21	-56.15	0.31	0.35	61	55
T10→C	-53.42	-55.51	0.53	0.56	65	58
T11→C	-56.96	-56.13	0.36	0.32	74	56
T12→C	-55.04	-55.99	0.30	0.67	71	57
T13→C	-57.74	-55.83	0.10	0.52	68	58
T14→C	-55.99	-55.69	0.13	0.59	66	52
T15→C	-55.13	-55.14	0.29	0.69	64	55
T16→C	-55.63	-55.23	0.08	0.50	64	54